

## Collection of transverse and longitudinal fields by means of apertureless nanoprobes with different metal coating characteristics

E. Descrovi,<sup>a)</sup> L. Vaccaro, W. Nakagawa, L. Aeschimann,<sup>b)</sup> U. Stauffer, and H. P. Herzig  
*Institute of Microtechnology, University of Neuchâtel, Rue A.-L. Breguet 2 and Rue Jaquet Droz 1,  
2000 Neuchâtel, Switzerland*

The coupling and transmission of transverse and longitudinal fields into apertureless microfabricated near-field optical probes is investigated. Two kinds of probes with different metal coating roughness are considered. Transverse and longitudinal field distributions are obtained by focusing azimuthally and radially polarized beams produced by means of a liquid crystal plate. The focal plane is scanned using microfabricated probes in a collection mode configuration. It is found that the roughness of the metal coating plays an important role in the coupling strength of transverse fields into the probes: the relative coupling efficiency for transverse fields diminishes with a rough metal coating, while that of longitudinal fields does not.

Near-field scanning systems can map optical fields by locally probing small regions of space with suitable nanoprobes. Two of the most well-established scanning near-field optical microscopy (SNOM) techniques make use of probes consisting of metal-coated tapered fibers (or tapered glass capillaries) used as light collectors<sup>1</sup> or metal (or silicon) tips used as light scatterers.<sup>2</sup> In mesoscopic optics, the electromagnetic field must be considered in its full vectorial nature and, in order to experimentally obtain complete information on the field amplitude, all three orthogonal components of the electric field vector must be accessible at each step of the scan. Therefore it is necessary to understand the interaction of the probe with not only the transverse components of the field, but also the component oriented longitudinally with respect to the tip axis.

In several experiments it has been found that the probe characteristics in imaging transverse and longitudinal fields differ. For example, in the work of Bouhelier *et al.*,<sup>3</sup> the behavior of metallic and dielectric probes in a scattering experiment is presented. It was found that gold tips are more likely to scatter longitudinally polarized fields, while uncoated glass probes are more sensitive to transversely polarized fields. With the advent of micro-machining technology, it has become possible to develop new batch fabrication processes for cantilever-based apertureless SNOM probes.<sup>4,5</sup> The micro-fabricated SNOM probes under consideration have been studied and characterized as light emitters in theoretical and experimental works.<sup>6,7</sup> It has been suggested that a longitudinally polarized field confined in a small volume at the probe apex can be generated when a radially polarized mode is guided into the conical structure of the probe. The importance of such a longitudinal field in the resolution capabilities of SNOM systems has been widely demonstrated.<sup>8,9</sup> In this letter, the coupling of longitudinally and transversely polarized fields into a microfabricated probe working in collection mode is investigated for probes with differing metal coating roughness.

Longitudinally and transversely polarized fields can be generated by focusing radially and azimuthally polarized beams. Their main feature is a space-variant polarization distribution with rotational symmetry around the propagation axis. Such axially symmetric beams can be produced in several ways (see for example Refs. 10 and 11). In our experiment, a  $\theta$ -cell polarization converter as described in Refs. 12 and 13 is employed. The cell is made of a linearly and a circularly rubbed alignment layer filled with nematic liquid crystals (LC). The light exiting from the  $\theta$ -cell has an electric field vector oriented either radially or azimuthally. Nonetheless, the  $\theta$ -cell does not provide the necessary phase arrangement to obtain a circularly symmetric focal plane pattern. In order to verify this aspect, calculations based on the method proposed by Mansuripur<sup>14,15</sup> were performed. Results, shown in Fig. 1, correspond to an azimuthally and a radially polarized beam generated by an ideal  $\theta$ -cell illuminated by a linearly polarized TEM<sub>00</sub> beam and focused by an aplanatic thin lens having numerical aperture (N.A.) equal to 0.65. The phase function of the  $\theta$ -cell is defined according to the orientation of the LC molecules in the cell. The focused azimuthally polarized beam has an electric field vector that is always transverse with respect to the propagation axis [Fig. 1(a)], while the focused radially polarized beam has both transverse [Fig. 1(b)] and longitudinal [Fig. 1(c)] electric field components. Note that the intensities of the transverse field for both the radially and the azimuthally polarized beam have the same pattern.

The device used to probe the near field is a hybrid SNOM/AFM (atomic force microscope). Specifically, it is a static AFM used as a collection-mode SNOM working in transmission. The light source is an Ar<sup>+</sup> laser of 514.5 nm wavelength. The light passes through the LC  $\theta$  cell and is then focused close to the tip by an objective (N.A.=0.65) mounted on the xyz-piezo stage (Piezo Flexure Stage P-517.3CL). The tip axis and the optical axis of the objective are aligned. The SNOM probes consist of a 12  $\mu$ m-long amorphous SiO<sub>2</sub> conical structure fabricated on silicon cantilevers and completely coated with a polycrystalline aluminum layer having a thickness of approximately 60 nm. In the first kind of probe considered (called a *standard probe* in the

<sup>a)</sup>Electronic mail: emiliano.descrovi@unine.ch

<sup>b)</sup>Also at: the Swiss Center for Electronics and Microtechnology CSEM, Rue Jaquet-Droz 1, 2007 Neuchâtel, Switzerland.

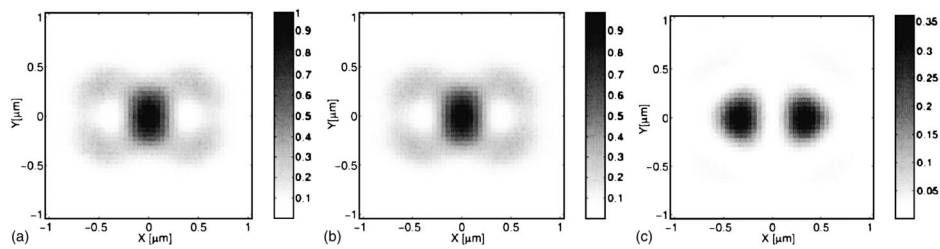


FIG. 1. Calculated patterns of axially symmetric beams as produced by an ideal  $\theta$  cell and focused with a N.A. = 0.65 aplanatic lens. (a) Azimuthally polarized beam: total intensity, (b) radially polarized beam: transverse field intensity, (c) radially polarized beam: longitudinal field intensity. All the pictures are normalized to the maximum value of the total intensity.

following), aluminum is deposited in the step-coverage mode.<sup>16</sup> In the transmission electron microscope (TEM) image [Fig. 2(a)] it is possible to note the presence of metal grains. The estimated mean roughness of the metal surface is  $1.9 \text{ nm} \pm 0.5 \text{ nm}$ .

In the second kind of probe, the quartz core is the same as in the standard probe, but the metal coating is deposited perpendicular to the wafer surface (*normal mode*). In Fig. 2(b) a TEM image of this probe is presented. The layer surface exhibits a much higher roughness (estimated to be equal to  $5.5 \text{ nm} \pm 0.5 \text{ nm}$ ), principally due to the different growth process of metal clusters on the quartz. The overall effect is a disordered distribution of small metal grains. In the following, this probe will be referred to as a *rough probe*. It is interesting to note that at the very end of the tip, a large metal grain can be found, as is the case with the standard probe. The light coupled into either probe is transmitted through the quartz core. A square hole in the cantilever, located underneath the tip base, allows the light to pass through. Some collection lenses produce an image of the hole in the photocathode plane of a photomultiplier (Perkin Elmer MD-952).

The position of the focal plane of the objective with respect to the probe is determined by scanning the focal region in the  $z$  direction, searching for the maximum detected intensity. The scans are then performed by driving the piezo at a constant value of  $z$ . The setup allows switching from radial to azimuthal polarization by rotating the polarization of the input beam by  $90^\circ$ , and ensures the maximum stability to the system. The area of the scans was generally  $2 \mu\text{m} \times 2 \mu\text{m}$  (pixel size approximately equal to  $16 \text{ nm}$ ).

In Fig. 3 the intensity distributions of focused azimuthally and radially polarized beams as imaged by the SNOM using a standard probe are shown. In the case of the focused azimuthally polarized beam, the recorded image [Fig. 3(a)] is very similar to the calculated one, shown in Fig. 1(a). As expected, the tip has collected the transverse field, the only field present in the focal plane. For the focused radially polarized beam, the total field intensity distribution is given by the sum of the transverse and the longitudinal fields shown in

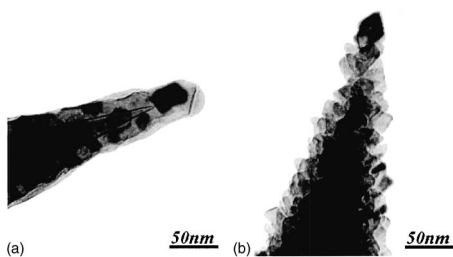


FIG. 2. Transmission electron microscopy images of the apex of quartz tips aluminum coated: (a) standard probe (metal deposition in step-coverage mode), (b) rough probe (metal deposition in normal mode).

Figs. 1(b) and 1(c). However, if the relative collection efficiency of the two fields into the tip is significantly different, then the measured image would be closer to one of the two patterns. Figure 3(b) clearly shows that this is the case: the detected field is more similar to the transverse field distribution than the longitudinal one. It can be noted that the central spot is a bit broader as compared to the azimuthal case, suggesting that the contribution of the two lobes of the longitudinal field are weak but present. This indicates that there is a much stronger transmission of the transverse field into the probe, but the present measurements do not permit an exact determination of the relative strength of this coupling.

A second set of measurements has been performed using a rough probe. In Fig. 4(a) the image of the focused azimuthally polarized beam is shown. In this case the field is purely transverse and the recorded pattern is similar to the one obtained with a standard probe. The image of the focused radially polarized beam is depicted in Fig. 4(b). This pattern is clearly not similar to either the transverse field intensity of Fig. 1(b) or the total field intensity given by the sum of the patterns in Figs. 1(b) and 1(c). Rather, the detected image is most similar to the intensity distribution of the longitudinal component only. By comparing the dimensions and the positions of the lobes in the measured image with the calculations, it is possible to conclude that the rough probe has

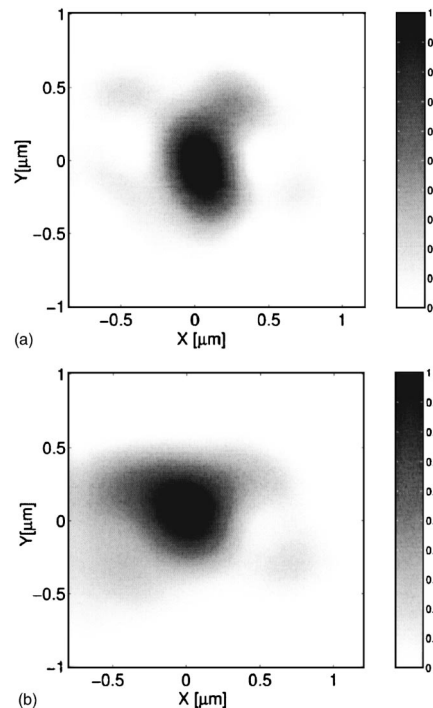


FIG. 3. Intensity distribution of a focused (a) azimuthally polarized beam and (b) radially polarized beam as imaged by the SNOM with a standard probe.

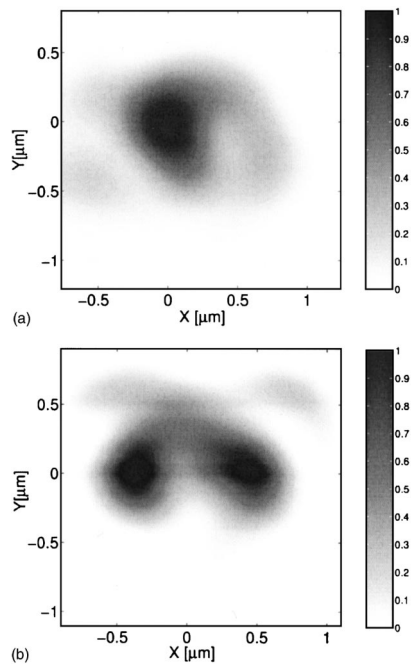


FIG. 4. Intensity distribution of focused (a) azimuthally polarized beam and (b) radially polarized beam as imaged by the SNOM with a rough probe.

mainly transmitted the longitudinally oriented component of the field while the transverse component has been blocked.

As a confirmation of this effect with the rough probe, a scan over a plane  $2 \mu\text{m}$  away from the focal plane has been performed. In this plane, the field for both the azimuthal and the radial beams is expected to be purely transverse. In fact, images of the the azimuthally [Fig. 5(a)] and the radially polarized [Fig. 5(b)] beams are very similar. The two lobes due to the longitudinal field are no longer observed.

An explanation of the filtering of the transverse field can be found by considering the waveguiding properties of the probe studied in illumination mode.<sup>6</sup> The conical geometry of the probe can guide two different kinds of mode having linear or radial polarization. The radial mode is guided to the very end of the tip, while the linearly polarized mode reaches cut-off in the tapered section of the probe, and either leaks through the metal layer or is reflected. Even if the collection mode and illumination mode situations are not exactly equivalent, it is reasonable to suppose that in collection mode a transverse field (i.e., a locally linearly polarized field) will be coupled into the tip where its dimensions allow the transverse linearly polarized mode to be guided, while a longitudinal field will be coupled close to the apex. With the rough probe we believe that the significant roughness of the lateral surface impedes the collection of the transverse component of the field, while leaving more or less unaffected the coupling of the longitudinal component at the apex. Since the transverse and the longitudinal fields are collected in spatially different places of the probe, there is also expected to be a difference in the optical resolution for the two polarizations.

A study on the light-collection properties of apertureless microfabricated quartz probes has been presented. Transversely and longitudinally polarized fields, produced by focusing a radially polarized beam, are imaged by two kinds of probes: standard and rough. It has been demonstrated that,

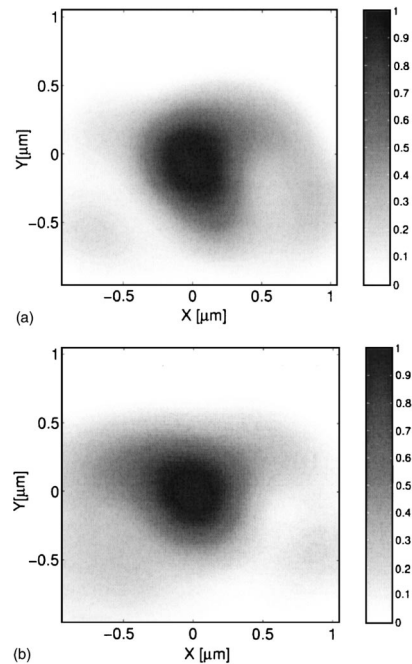


FIG. 5. Intensity distribution of focused (a) azimuthally polarized beam and (b) radially polarized beam as imaged by the SNOM with a rough probe. The scans are performed on a plane  $2 \mu\text{m}$  away from the focus.

with apertureless SNOM probes used in collection mode, it is possible to access the longitudinal, nonpropagating fields confined in the focal region of a lens. By comparing measurements with theoretical results, it is possible to underline the importance of the metal coating roughness in blocking the transverse component of the field, and gain some insight into the collection mechanism of three-dimensional optical fields in such probes.

T.S. and I.P. are gratefully acknowledged for the preparation of the liquid crystal element used in the experimental setup. This work has been supported by E. U. Grant No. IST-2000-26479, the Swiss National Science Foundation, and the program TOP NANO 21.

- <sup>1</sup>E. Betzig, M. Isaacson, and A. Lewis, *Appl. Phys. Lett.* **51**, 2088 (1987).
- <sup>2</sup>F. Zenhausern, M. P. O'Boyle, and H. K. Wickramasinghe, *Appl. Phys. Lett.* **65**, 1623 (1994).
- <sup>3</sup>A. Bouhelier, M. R. Beversluis, and L. Novotny, *Appl. Phys. Lett.* **82**, 4596 (2003).
- <sup>4</sup>G. Schürmann, W. Noell, U. Staufer, N. F. de Rooij, R. Eckert, J. M. Freyland, and H. Heinzelmann, *Appl. Opt.* **40**, 5040 (2001).
- <sup>5</sup>R. Eckert, J. M. Freyland, H. Gersen, H. Heinzelmann, G. Schürmann, W. Noell, U. Staufer, and N. F. de Rooij, *Appl. Phys. Lett.* **77**, 3695 (2000).
- <sup>6</sup>L. Vaccaro, L. Aeschimann, U. Staufer, H. P. Herzig, and R. Dändliker, *Appl. Phys. Lett.* **83**, 584 (2003).
- <sup>7</sup>L. Aeschimann, T. Akiyama, U. Staufer, N. F. de Rooij, L. Thiery, R. Eckert, and H. Heinzelmann, *J. Microsc.* **209**, 182 (2003).
- <sup>8</sup>L. Novotny, E. J. Sanchez, and X. S. Xie, *Ultramicroscopy* **71**, 21 (1998).
- <sup>9</sup>L. Aeschimann, L. Vaccaro, T. Akiyama, U. Staufer, N. F. de Rooij, R. Eckert, and H. Heinzelmann, *AIP Conf. Proc.* **696**, 906 (2003).
- <sup>10</sup>Z. Bomzon, V. Kleiner, and E. Hasman, *Appl. Phys. Lett.* **79**, 1587 (2001).
- <sup>11</sup>U. Levy, C. Tsai, L. Pang, and Y. Fainman, *Opt. Lett.* **29**, 1718 (2004).
- <sup>12</sup>M. Stalder and M. Schadt, *Mol. Cryst. Liq. Cryst. Sci. Technol., Sect. A* **282**, 343 (1996).
- <sup>13</sup>S. Masuda, T. Nose, R. Yamaguchi, and S. Sato, *Proc. SPIE* **2873**, 301 (1996).
- <sup>14</sup>M. Mansuripur, *J. Opt. Soc. Am. A* **3**, 2086 (1986).
- <sup>15</sup>M. Mansuripur, *J. Opt. Soc. Am. A* **6**, 786 (1989).
- <sup>16</sup>M. Madou, *Fundamentals of Microfabrication* (CRC Press, Boca Raton, FL, 1997).